The emergence of spin electronics in data storage

Electrons have a charge and a spin, but until recently these were considered separately. In classical electronics, charges are moved by electric fields to transmit information and are stored in a capacitor to save it. In magnetic recording, magnetic fields have been used to read or write the information stored on the magnetization, which 'measures' the local orientation of spins in ferromagnets. The picture started to change in 1988, when the discovery of giant magnetoresistance opened the way to efficient control of charge transport through magnetization. The recent expansion of hard-disk recording owes much to this development. We are starting to see a new paradigm where magnetization dynamics and charge currents act on each other in nanostructured artificial materials. Ultimately, 'spin currents' could even replace charge currents for the transfer and treatment of information, allowing faster, low-energy operations: spin electronics is on its way.

CLAUDE CHAPPERT[1,2]*, ALBERT FERT[2,3] AND FRÉDÉRIC NGUYEN VAN DAU[2,3]

[1]Institut d'Electronique Fondamentale, CNRS, UMR8622, 91405 Orsay, France
[2]Université Paris Sud, 91405 Orsay, France
[3]Unité Mixte de Physique CNRS-Thales, 91767 Palaiseau, France
*e-mail: claude.chappert@ief.u-psud.fr

The interdependence between magnetization and charge transport is not a new story. For instance, anisotropic magnetoresistance (AMR), which links the value of the resistance to the respective orientation of magnetization and current, was first observed in 1856 by William Thomson, but its amplitude is weak (up to a few per cent variation in resistance on changing the relative orientation of magnetization and current). Nevertheless, the introduction by IBM in 1991 of a magnetoresistive read head based on AMR was a major technological step forward[1]. In hard disk drives (HDD), the head flies at constant height above the magnetic domains that define the 'bits' in the recording medium, and senses the spatial variations of the stray magnetic field of these domains. The old ring-shaped magnetic head, invented in 1933 by Eduard Schuller (AEG) for tape recording, measured a magnetic flux, and so was approaching its sensitivity limit with the reduction of the head dimensions. In the IBM head (Fig. 1), the AMR sensor is combined with a 'ring' element still used for writing, and directly senses the magnetic field through its influence on the magnetization orientation in the head. The AMR head had a relative 'magnetoresistance' (hereafter referred to as $\Delta R/R = (R_{max} - R_{min})/R_{min}$) of the order of only 1%, but this was enough to increase the growth rate of HDD storage areal density from 25% per year, its value since nearly the introduction of HDD in 1957, up to 60% per year.

FUNDAMENTALS OF SPIN ELECTRONICS

The physics behind today's fast expansion of spin electronics has also been known for a long time. A cornerstone is the 'two currents' conduction concept proposed by Mott[2] and used by Fert and Campbell[3,4] to explain specific behaviours in the conductivity of the ferromagnetic metals Fe, Ni, Co and their alloys. In such 'itinerant ferromagnets' both the 4s and 3d electron bands contribute to the density of states at the Fermi level E_F. Because of the strong exchange interaction favouring parallel orientation of electron spins, the 'spin-up' and 'spin-down' 3d bands are shifted in energy. This band splitting creates the imbalance between numbers n_{up} and n_{down} of 3d electrons that is at the origin of the ferromagnetic moment ($\mu \approx -(n_{up} - n_{down})\mu_B$/atom, where μ_B is the Bohr magneton), whereas the conduction is dominated by the unsplit 4s band, the 4s electrons having a much higher mobility. However, the spin-conserving s-to-d transitions are the main source of s-electron scattering. This has two chief consequences for transport: the spin-imbalanced density of states for 3d electrons at E_F results in strongly spin-dependent scattering probabilities (Fermi 'Golden Rule'), and between two spin-flip scattering events an electron can undergo many scattering events that keep the same spin direction. Thus at the limit where spin-flip scattering events are negligible, conduction happens in parallel through two spin channels that have very different conductivities.

Important length scales can be discussed in the diffusive transport model. The spin-dependent scattering probability results in very different mean free paths λ_{up} and λ_{down}, or equivalently relaxation times τ_{up} and τ_{down}. In usual thin metallic layers they scale from a few nanometres to a few tens of nanometres, with highly variable $\lambda_{down}/\lambda_{up}$ ratios: some impurities have strongly spin-dependent cross-sections, so that in Ni, for example, the ratio $\lambda_{down}/\lambda_{up}$ can reach 20 for
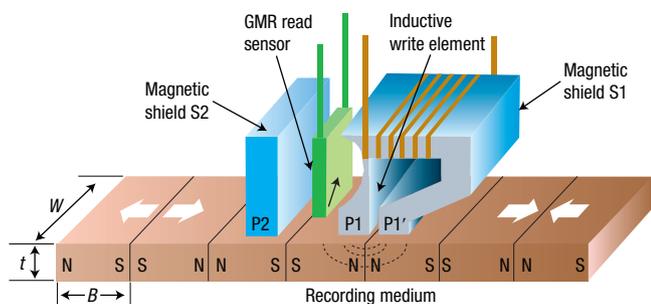
Figure 1 Magnetoresistive head for hard-disk recording. Schematic structure of the magnetoresistive head introduced by IBM for its hard disk drives in 1991. A magnetic sensor based on anisotropic magnetoresistance (left) is added to the inductive 'ring-type' head (right) still used for writing. The distances P1–P1′ and P1–P2 between the pole pieces of the magnetic shields S1 and S2 define respectively the 'write' and 'read' gaps, on which depends the minimum length B of the magnetic domains. W is the track width and t is the thickness of the recording medium. Note that in today's hard disk recording, W and B are of the order of 100 nm and 30 nm respectively, but with a different arrangement of head and domains in 'perpendicular recording'[1].

Co impurities or decrease to 0.3 with Cr doping[4]. Another important length scale is the spin-conserving drift length projected along one direction, called the spin diffusion length L_{sf} (sf denotes spin flip). It is generally much larger than the mean free path[5].

GIANT MAGNETORESISTANCE AND THE SPIN-VALVE HEAD

The founding step of spin electronics, which triggered the discovery of the giant magnetoresistance[6,7], was actually to build magnetic multilayers with individual thicknesses comparable to the mean free paths, so that evidence could be seen for spin-dependent electron transport. The principle is schematized in Fig. 2 for the simplest case of a triple-layer film of two identical ferromagnetic layers F1 and F2 sandwiching a non-magnetic metal spacer layer M, when the current circulates 'in plane' (cf. Fig. 2b). We assume $\lambda^F_{up} \gg \lambda^F_{down}$, with $\lambda^F_{up} > t_F > \lambda^F_{down}$, for the thickness t_F of the magnetic layer and $t_M \ll \lambda_M$ for the thickness t_M of the spacer layer. When the two magnetic layers are magnetized parallel (P), the spin-up electrons can travel through the sandwich nearly unscattered, providing a conductivity shortcut and a low resistance. On the contrary, in the antiparallel (AP) case, both spin-up and spin-down electrons undergo collisions in one F layer or the other, giving rise to a high resistance. The relative magnetoresistance $\Delta R/R = (R_{AP} - R_P)/R_P$ can reach 100% or more in multilayers with a high number of F/M periods. It was already 80% in the Fe/Cr multilayer of the original discovery[6], hence the name of giant magnetoresistance (GMR). Elaborate theories must of course take into account other effects such as interfacial scattering and quantum confinement of the electrons in the layers[8,9]. The GMR is an outstanding example of how structuring materials at the nanoscale can bring to light fundamental effects that provide new functionalities. And indeed the amplitude of the GMR immediately triggered intense research, soon achieving the definition of the spin-valve sensor[10–12]. In its simplest form, the spin valve is just a trilayer film of the kind displayed in Fig. 2a in which one layer (for example, F2) has its magnetization pinned along one orientation. The rotation of the free F1 layer magnetization then 'opens' (in P configuration) or 'closes' (in AP configuration) the flow of electrons, acting as a sort of valve.

The standard spin valve shows magnetoresistance values of about 5–6%. More complex spin-valve stacks, with layer thicknesses

controlled at the atomic scale and ultra-low surface roughness, are optimized to favour specular reflection of electrons towards the active part so that the magnetoresistance reaches about 20%. Following the introduction in 1997 by IBM of the spin-valve sensor (Fig. 2b) to replace the AMR sensor in magnetoresistive HDD read heads, the growth rate for storage areal density immediately increased up to 100% per year. Together, the sequential introduction of the magnetoresistance and spin-valve head, by providing a sensitive and scalable read technique, contributed to increase the raw HDD areal recording density by three orders of magnitude (from ~0.1 to ~100 Gbit in^{-2}) between 1991 and 2003. This jump forward opened the way both to smaller HDD form factors (down to 0.85-inch disk diameter) for mobile appliances such as ultra-light laptops or portable multimedia players, and to unprecedented drive capacities (up to a remarkable 1 terabyte) for video recording or backup. HDDs are now replacing tape in at least the first tiers of data archival strategies, for which they provide faster random access and higher data rates. However, the areal density growth rate started to slow down after 2003, when other problems joined the now limiting spin-valve head.

Attempts were also made to develop solid-state magnetic storage. Provided that the free layer magnetization of the spin valve is constrained to take only the two opposite orientations of an easy magnetization axis, arrays of patterned spin-valve elements can be used to store binary information with resistive read-out. Spin-valve solid-state memories were indeed developed[13]. But the planar geometry of the spin-valve sensor intrinsically limits the integration into high-density nanoelectronics, and the low metallic resistance and $\Delta R/R$ value around 10% are not well adapted to CMOS electronics. For read heads also, the 'current in plane' spin-valve geometry is a limitation to the downscaling. First, it is easy to see that the integration of the planar element of Fig. 2b between the magnetic shields of the read head of Fig. 1 strongly limits the minimum dimension of the read gap between the P1 and P2 poles, a crucial requirement for reducing the bit length: indeed, two thick insulating layers are needed on either part of the sensor. The 'current perpendicular to plane' (CPP) geometry of Fig. 2c is much better for this purpose, as the spin-valve sensor can be directly connected to the magnetic shields. This configuration is also more favourable for reducing the track width.

Simple geometrical arguments based on the average electron propagation direction also lead us to expect higher magnetoresistance values for a spin valve in the CPP configuration. The fundamental study of CPP GMR was indeed extremely productive in terms of the new concepts of spin injection and spin accumulation[14]. The basic principle is displayed in Fig. 3. Again we assume that $\tau_{up} \gg \tau_{down}$ in the ferromagnetic metal. So when a current flows from a ferromagnetic layer (F) to a non-magnetic layer (N), away from the interface the current densities j_{up} and j_{down} must be very different on the ferromagnetic side, and equal on the non-magnetic side. The necessary adjustment requires that, in the area near the interfaces, more electrons from the spin-up channel flip their spins. This occurs through an 'accumulation' of spin-up electrons, that is, a splitting of the E_{Fup} and E_{Fdown} Fermi energies, which induces spin-flips and adjusts the incoming and outgoing spin fluxes. The spin-accumulation decays exponentially on each side of the interface on the scale of the respective spin diffusion lengths L^F_{sf} and L^N_{sf}. In this spin accumulation zone, the spin polarization of the current decreases progressively going from the magnetic conductor to the non-magnetic one, so that a spin-polarized current is 'injected' into the non-magnetic metal up to a distance that can reach a few hundreds of nanometres, well beyond the ballistic range. This concept has been extended to more complex interfaces between metals and semiconductors[15] (Fig. 3c). Likewise, the concept applies when an interfacial resistance such as a Shottky or insulating barrier exists[16]. The spin-injection effect has also been demonstrated for
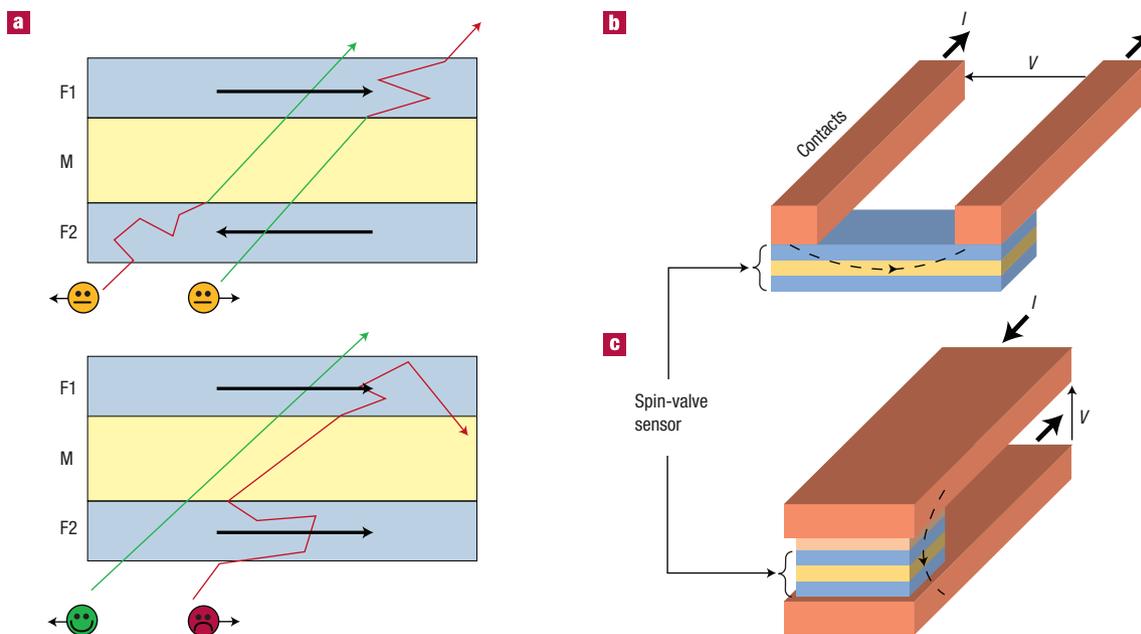
Figure 2 The spin valve. **a**, Schematic representation of the spin-valve effect in a trilayer film of two identical ferromagnetic layers F1 and F2 sandwiching a non-magnetic metal spacer layer M, the current circulating in plane. When the two magnetic layers are magnetized parallel (lower scheme), the spin-up electrons (spin antiparallel to the magnetization) can travel through the sandwich nearly unscattered, providing a conductivity shortcut and a low resistance. In contrast, in the antiparallel case (top scheme) both spin-up and spin-down electrons undergo collisions in either F1 or F2, giving rise to a higher overall resistance. **b**, Schematic arrangement of the 'current in plane' spin-valve sensor in a read head. **c**, Schematic arrangement of the 'current perpendicular to plane' spin-valve sensor in a read head. In both configurations, the recording medium travels parallel to the front face of the sensor.

planar geometries[17], and proposed for use in three-terminal devices such as the spin transistor[18]. We will come back to this point later.

If the magnetoresistance ratio is larger in the CPP geometry, exceeding 20%, CPP GMR samples are much more difficult to fabricate[19]. In particular, quantitative measurements require either superconducting contacts[20] or long multilayered wires[21] to ensure current lines perpendicular to the layers. And the resistance and magnetoresistance still remain too small for optimal application to read heads[22]. Considerable industrial research is going on (see for instance ref. 23).

MAGNETIC TUNNEL JUNCTION

Another big step forward came from replacing the non-magnetic metallic spacer layer M of the spin valve by a thin (~1–2 nm) non-magnetic insulating layer, thus creating a magnetic tunnel junction (MTJ). In that configuration the electrons travel from one ferromagnetic layer to the other by a tunnel effect, which conserves the spin (Fig. 4a). Again, this is not a new story, as it was proposed by Jullière[24] in 1975, but its practical realization with a high magnetoresistance (up to 30% at 4.2 K) had to wait until 1995 once considerable progress had been made in deposition and nanopatterning techniques[25,26]. The first MTJs used an amorphous Al_2O_3 insulating layer between ferromagnetic metal layers: the tunnel magnetoresistance (TMR) of such stacks reached a limit around 70% at room temperature. Much higher effects were later obtained with a single-crystal MgO barrier[27,28]. Within such a barrier, the tunnelling current is carried by evanescent waves of several well-defined symmetries, which, at least for high-quality interfaces, have an interfacial connection in the metals only to Bloch waves of the same symmetry at the Fermi level[29,30]. In the typical case of MgO(001) between Co electrodes for instance,

the decay is much slower and the transmission higher for the evanescent waves of symmetry Δ_1, so that the TMR comes from the specific high spin polarization of the states of symmetry Δ_1 in a zone of the Fermi surface of Co near [001]. The MgO barrier is thus 'active' in selecting a symmetry of high spin polarization, leading to latest record values of $\Delta R/R = 1010\%$ at 5 K, 500% at room temperature (Fig. 4b)[31]. There is no sharp symmetry selection in amorphous barriers such as Al_2O_3, which explains the much lower TMR ratios achieved.

The magnetic tunnel junction is clearly a CPP 'vertical' device, with a magnetic behaviour similar to a spin valve but magnetoresistance values up to two orders of magnitude higher. It is stable up to reasonable breakdown voltages (above 1 V), and the equipment suppliers rapidly developed reliable techniques to scale down its dimensions to well below 100 nm. So its development had an immediate impact on storage applications. Indeed, a TMR read head was commercialized by Seagate[32] in 2005 (Fig. 4c), providing a higher sensitivity. This may prove to be a short-lived option: MTJs have an intrinsic high resistance (with resistance–area products above 1 Ω cm²), and with further downscaling it will become difficult to maintain a high signal-to-noise ratio with an increasing sensor resistance. Then CPP spin valves or degenerate MTJs could become more favourable[22].

MAGNETIC RANDOM ACCESS MEMORY

The 'high' MTJ resistance is actually more adapted to nanoelectronics. The 1995 publications started a race to develop the magnetic random access memory, or MRAM[13]. Figure 5a shows the principle of this magnetic solid state memory, in the basic 'cross point' architecture. The binary information 0 and 1 is recorded on the two opposite orientations of the magnetization of the free layer along its easy magnetization axis. The MTJs are
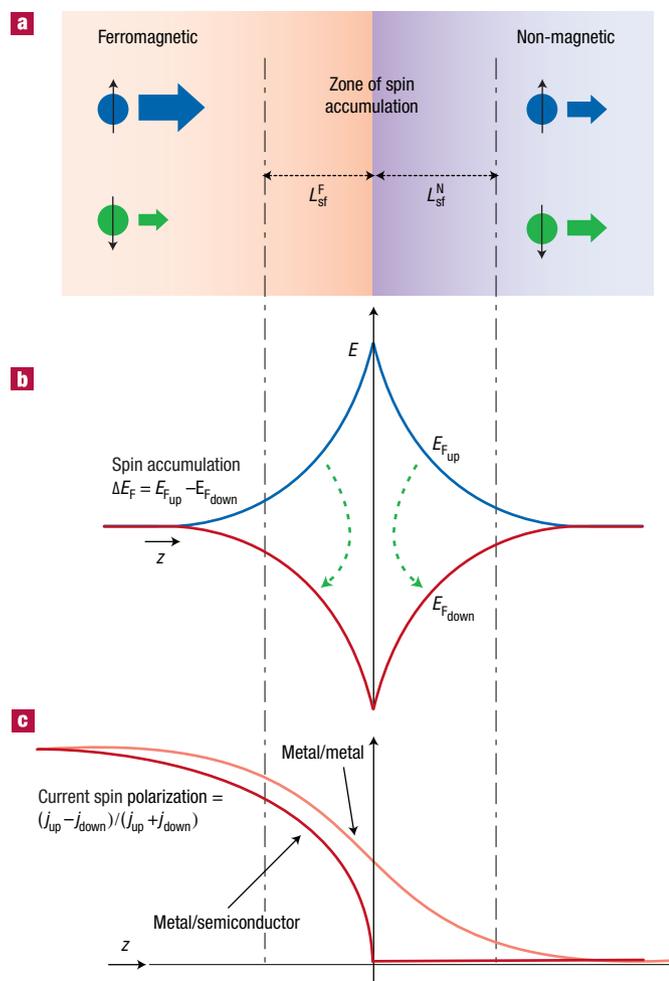
Figure 3 Spin accumulation. Schematic representation of the spin accumulation at an interface between a ferromagnetic metal and a non-magnetic layer, adapted from ref. 132. **a**, Spin-up and spin-down current far from an interface between the ferromagnetic and nonmagnetic conductors (outside the spin-accumulation zone). L_{sf}^F and L_{sf}^N are, respectively, the spin diffusion lengths in the ferromagnetic and non-magnetic layers. **b**, Splitting of the Fermi levels $E_{F\,up}$ and $E_{F\,down}$ at the interface. The dashed green arrows symbolize the transfer of current between the two channels by the unbalanced spin flips caused by the out-of-equilibrium spin-split distribution, which governs the depolarization of the electron current between the left and the right. With the current in the opposite direction, there is an inversion of the spin accumulation and opposite spin flips, which polarizes the current across the spin-accumulation zone. **c**, Variation of the current spin polarization when there is an approximate balance between the spin flips on both sides (metal/metal) and when the spin flips on the left side are predominant (metal/semiconductor, for example). The current densities for spin-up and spin-down electrons are j_{up} and j_{down}, respectively.

connected to the crossing points of two perpendicular arrays of parallel conducting lines. For writing, current pulses are sent through one line of each array, and only at the crossing point of these lines is the resulting magnetic field high enough to orient the magnetization of the free layer. For reading, the resistance between the two lines connecting the addressed cell is measured. In principle, this cross point architecture promises very high densities. In practice, the amplitude of magnetoresistance remains too low for fast, reliable reading because of the unwanted current paths as well as the direct one through the addressed cell. So,

realistic cells add one transistor per cell, resulting in more complex 1T/1MTJ cell architectures such as the one represented in Fig. 5b. Several demonstrator circuits were rapidly presented by most leading semiconductor companies, culminating with the first MRAM product, a 4-Mbit stand-alone memory[33] commercialized by Freescale in 2006 (Fig. 5c), and voted 'Product of the Year' by *Electronics Products Magazine* in January 2007.

The MRAM potentially combines key advantages such as non-volatility, infinite endurance and fast random access (down to 5 ns read/write time[34]) that make it a likely candidate for becoming the 'universal memory', one of the chief aims of nanoelectronics. Such a memory is able to provide data/code (Flash, ROM) and execution (DRAM, SRAM) storage using a single memory technology on the same die. Moreover, in June 2007 Freescale introduced a new version able to work in the expanded temperature range of –40 °C to 105 °C, thus qualifying for military and space applications where the MRAM will also benefit from the intrinsic resistance to radiation of magnetic storage.

NANOMAGNETISM

Progress in spin electronics cannot be separated from the development of 'nanomagnetism'. In particular, the engineering of magnetic properties at atom level in multilayers was developed in parallel with GMR and helped to make it possible. Improved knowledge of the role of interface effects, and the use of the layer thickness as a parameter, led to the development of artificial magnetic materials with finely tuned new properties. This had a direct impact on spin storage.

The magnetic storage of binary information requires the engineering of an energy barrier between two opposite orientations of the magnetization, able to stop thermally excited reversals[35]. This 'magnetic anisotropy' has several competing origins. The strongest one is usually the shape anisotropy due to the dipole–dipole magnetic interaction, which induces the well-known in-plane easy magnetization of thin films. But the main effect used in recording is the magnetocrystalline anisotropy, an atomic effect correlated to the symmetry of the immediate atomic environment. The interface anisotropy, initially proposed by Néel[36], takes advantage of the break in translational symmetry at an interface to generate giant magnetic anisotropies, able to overcome the shape anisotropy and induce a stable perpendicular magnetization axis (PMA) in ultrathin films and multilayers. This PMA was first observed in 1967 on single-atomic-layer films[37], and achieved in 1985 in Co/Pd multilayer[38] and Au/Co/Au films[39] with more practical thicknesses. New materials could even be predicted from *ab initio* calculations[40]. PMA is now used for recording media in the 'perpendicular' HDD introduced by Seagate, Hitachi and Toshiba in 2005–06, which helped to restore the present 40% growth rate after the slow-down experienced in 2003–04.

Exchange bias is another crucial effect linked to an interface, here between a ferromagnetic and antiferromagnetic layer: the antiferromagnetic layer has no net magnetic moment that could be sensitive to an applied field, but may retain a large magnetic anisotropy, which, transferred to the ferromagnetic layer through interfacial exchange interaction, contributes to stabilizing the orientation of its magnetization. This is also an old story[41], but with progress in interface control[42] it gained wide application in the spin valve and magnetic tunnel junctions for pinning the magnetization of the reference magnetic layer. And it can also be used in a new kind of MRAM[43], or to fight thermal excitations of magnetic nanoparticles[44] for future storage.

The growing structural quality of interfaces has led to the spin-dependent quantum confinement of the electrons in metallic ultrathin layers. Together with interfacial band hybridization this
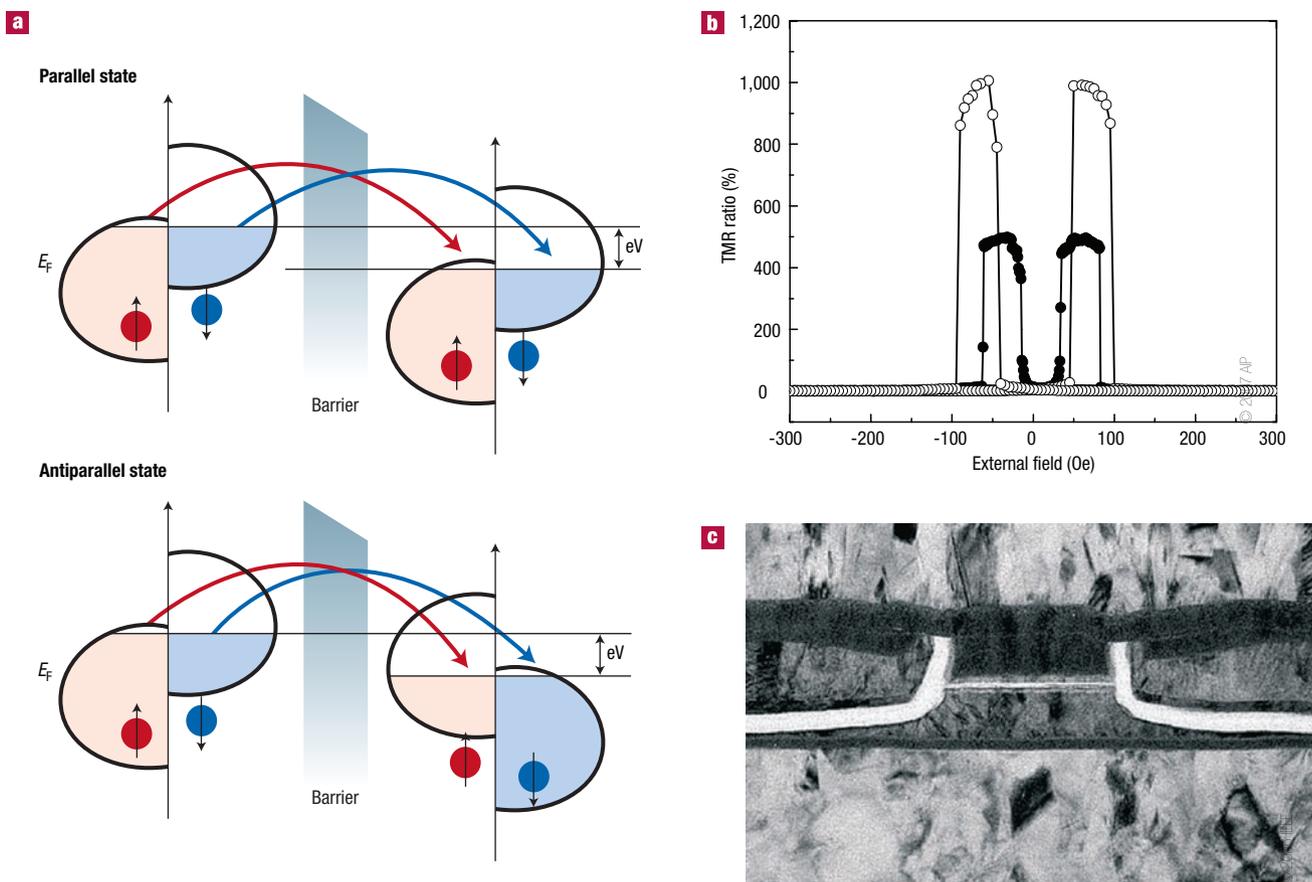
a

Parallel state

Antiparallel state

b

c

Figure 4 The magnetic tunnel junction. **a**, Schematic representation of the tunnel magnetoresistance in the case of two identical ferromagnetic metal layers separated by a non-magnetic amorphous insulating barrier such as Al_2O_3. The tunnelling process conserves the spin. When electron states on each side of the barrier are spin-polarized, then electrons will more easily find free states to tunnel to when the magnetizations are parallel (top picture) than when they are antiparallel (bottom picture). **b**, Record high magnetoresistance TMR $= (R_{max} - R_{min})/R_{min}$ for the magnetic stack $(Co_{25}Fe_{75})_{80}B_{20}$ (4 nm)/MgO (2.1 nm)/$(Co_{25}Fe_{75})_{80}B_{20}$ (4.3 nm) annealed at 475 °C after growth, measured at room temperature (filled circles) and at 5 K (open circles). Reprinted with permission from ref. 31. **c**, Transmission electron microscope cross-section of a TMR read head from Seagate. Reprinted with permission from ref. 32. The tunnel junction stack appears vertically at the centre of the picture, with the tunnel barrier at the level of the thin white horizontal line. The thick bent lines on both sides are the insulating layers between top and bottom contacts. The two thick light grey layers on top and bottom are the magnetic pole pieces (see Fig. 1). The track width of the TMR element is typically 90–100 nm.

now makes it possible to control the exchange interaction between ferromagnetic layers separated by a non-magnetic layer[45–49]. This, for instance, enables synthetic antiferromagnets (SAF) to be built, these being trilayers where two ferromagnetic layers are kept magnetized antiparallel by exchange through a non-magnetic spacer. Depending on their exact structure and properties, such SAFs can provide either improved non-volatility for constant writing field[50], or more reliable writing in solid state devices[51], or simply a weak sensitivity to applied field and minimal stray field when the net magnetic moment is brought to zero. They are thus used now as recording media for longitudinal HDD products[1] as well as in Freescale's MRAM product. And they are ubiquitous in all pinned layers of spin-valve sensors and MRAM cells where they help the exchange bias and minimize the interlayer dipole–dipole interaction.

So at the beginning of this century outstanding progress had been made both in designing the magnetic properties through atomic engineering, and in understanding and controlling the spin-dependent electron transport. And materials exist that allow thermally stable magnetic particles to be produced down to sizes of a few nanometres[52], seemingly opening a bright future for a high-density spin storage.

WRITING IS THE PROBLEM

The use of a magnetic field to write the information still remained a considerable limitation. This can easily be understood. Let us assume that information is stored in the form of the magnetization orientation of a nanoparticle of volume V. The energy barrier fighting the thermal excitations is given by KV, where K is the anisotropy constant per unit volume. Non-volatility — usually defined by a maximum error rate, for example 10^{-9}, over a 10-year period — is obtained when $KV > 50$–$60k_BT$, where k_B is the Boltzmann constant and T the temperature. So reducing V requires a corresponding increase in K, but then the writing field increases proportionally with K, whereas the power available to create it decreases as the dimensions are downscaled.

The problem is well known in HDD, where it was recently postponed by first introducing the SAF longitudinal media and then changing to perpendicular recording. The future also promises heat-assisted magnetic recording (HAMR)[1], where the magnetic field is helped by local heating of the media temporarily reducing the energy barrier, as in magneto-optical recording. But the fundamental limit is still there, together with other problems linked to the rotating nature
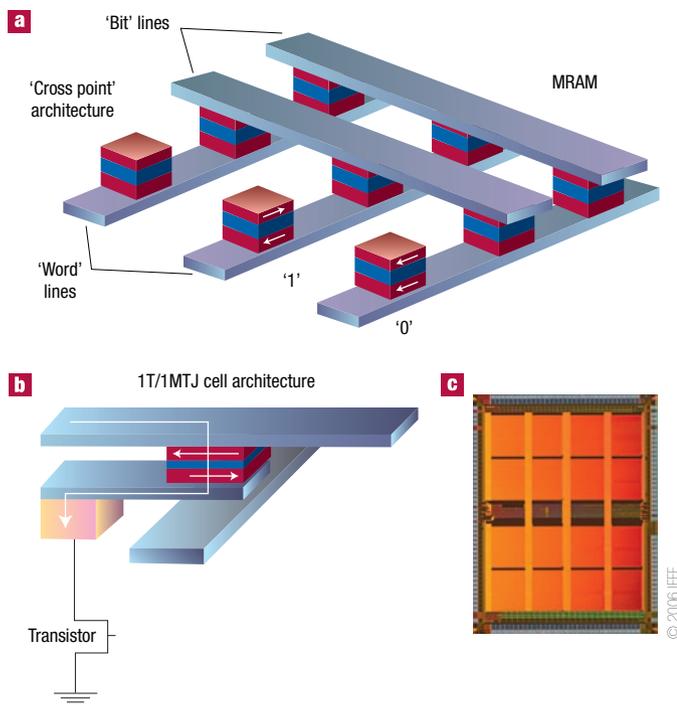
Figure 5 Magnetic random access memory. **a**, Principle of MRAM, in the basic cross-point architecture. The binary information 0 and 1 is recorded on the two opposite orientations of the magnetization of the free layer of magnetic tunnel junctions (MTJ), which are connected to the crossing points of two perpendicular arrays of parallel conducting lines. For writing, current pulses are sent through one line of each array, and only at the crossing point of these lines is the resulting magnetic field high enough to orient the magnetization of the free layer. For reading, the resistance between the two lines connecting the addressed cell is measured. **b**, To remove the unwanted current paths around the direct one through the MTJ cell addressed for reading, the usual MRAM cell architecture has one transistor per cell added, resulting in more complex 1T/1MTJ cell architecture such as the one represented here. **c**, Photograph of the first MRAM product, a 4-Mbit stand-alone memory commercialized by Freescale in 2006. Reprinted with permission from ref. 33.

of HDD storage such as mechanical tracking, slow access time (hardly reduced in several decades and still a few milliseconds) and energy consumption. The future markets of HDD, in particular through the competition with Flash storage, will depend on how such problems are solved. For instance, HDD currently maintains an areal density growth rate of roughly 40%, in line with Moore's law defining the minimum cell size of Flash. But meanwhile multi-level Flash cells have been introduced (2 bits per cell), and huge efforts have succeeded in reducing their cost.

In MRAM the writing problem was immediately worse than in HDD, as the conducting lines have much smaller dimensions, with a strong limitation in current density around 10^7 A cm^{-2} due to electromigration. Also, it is not possible in a very large-scale integration circuit to include an optimized 'ring-like' ferromagnetic circuit to 'channel' the magnetic induction to the magnetic media. A magnetic channelling was developed for MRAM[53], but the effect is limited (to a factor of about two) and requires costly fabrication steps. Finally, when approaching the downscaling limits the unavoidable distribution of writing parameters, coupled to the large stray fields in such densely packed arrays, leads to spreading program errors. Freescale researchers elegantly solved this reliability problem by

replacing the standard ferromagnetic free layer with a SAF layer, written using a spin-flop process[33,51,54], and this opened the way to the first MRAM product. But this is at the expense of higher writing currents (around 10 mA), and clearly limits the achievable densities and the downscaling. As for HDD, one solution could be heat-assisted recording (TAS-RAM)[43,55]. It was also proposed that writing could be assisted by microwave excitation at the ferromagnetic resonance frequency of the free layer[56–58], a technique that could also be useful for hard disks. But such promising techniques do not completely suppress the need for a magnetic field.

SPIN TRANSFER — A NEW ROUTE FOR WRITING MAGNETIC INFORMATION

The hoped for breakthrough for spin storage was provided by the prediction[59,60] in 1996 that the magnetization orientation of a free magnetic layer could be controlled by direct transfer of spin angular momentum from a spin-polarized current. In 2000, the first experimental demonstration that a Co/Cu/Co CPP spin-valve nanopillar can be reversibly switched by this 'spin-transfer effect' between its low (parallel) and high (antiparallel) magnetoresistance states was presented[61]. The concept of spin transfer actually dates back to the 1970s, with the prediction[62] and observations[63] of domain-wall dragging by currents. Spin-transfer effects had also been predicted[64] for MTJs as early as 1989. Somehow, those predictions did not immediately trigger the intense research work that followed the 1996 and 2000 publications, possibly because the required fabrication technologies were not mature enough.

The principle of 'spin-transfer torque' (STT) writing in nanopillars is shown schematically in Fig. 6a for the usual case of $3d$ ferromagnetic metals (for example Co) in a spin-valve structure with a non-magnetic metal spacer (for example Cu). Let us consider a 'thick' ferromagnetic layer F1, whereas the ferromagnetic layer F2 and the spacer M are 'thin' (compared with the length scales of spin-polarized transport[65]). F1 and F2 are initially magnetized along different directions. A current of s electrons flowing from F1 to F2 will acquire through F1, acting as a spin polarizer, an average spin polarization approximately along the magnetization of F1. When the electrons reach F2, the s–d exchange interaction quickly aligns the average spin moment along the magnetization of F2. In the process, the s electrons have lost a transverse spin angular momentum, which, because of the total angular momentum conservation law, is 'transferred' to the magnetization of F2. This results in a torque tending to align F2 magnetization towards the spin moment of the incoming electrons, and thus towards the magnetization of F1. Because the loss of transverse spin momentum happens over a very short distance (around 1 nm), the torque is an interfacial effect, more efficient on a thin layer. But a more important result is that the amplitude of the torque per unit area is proportional to the injected current density, so that the writing current decreases proportionally to the cross-sectional area of the structure. With today's advances in nanotechnologies and the easy access to sizes below 100 nm, this represents an important advantage of spin transfer over field-induced writing.

A realistic treatment of the effect[65] includes both quantum effects at the interfaces (spin-dependent transmission of Bloch states) and diffusive transport theory (spin-accumulation effects), and the dynamical behaviour can be studied through a modified Landau–Lifshitz–Gilbert equation describing the damped precession of magnetization in the presence of STT and thermal excitations[65,66]. The principle of STT writing of a MRAM cell is shown in Fig. 6b. Electrons flowing from the thick 'polarizing' layer to the thin free layer favour a parallel orientation of the magnetizations: if the initial state is antiparallel, then beyond a threshold current density j_{C+} the free layer will switch. When the electrons flow from the free to the polarizing layer, it can be shown that the effective spin moment injected in the free layer is opposed to the magnetization of
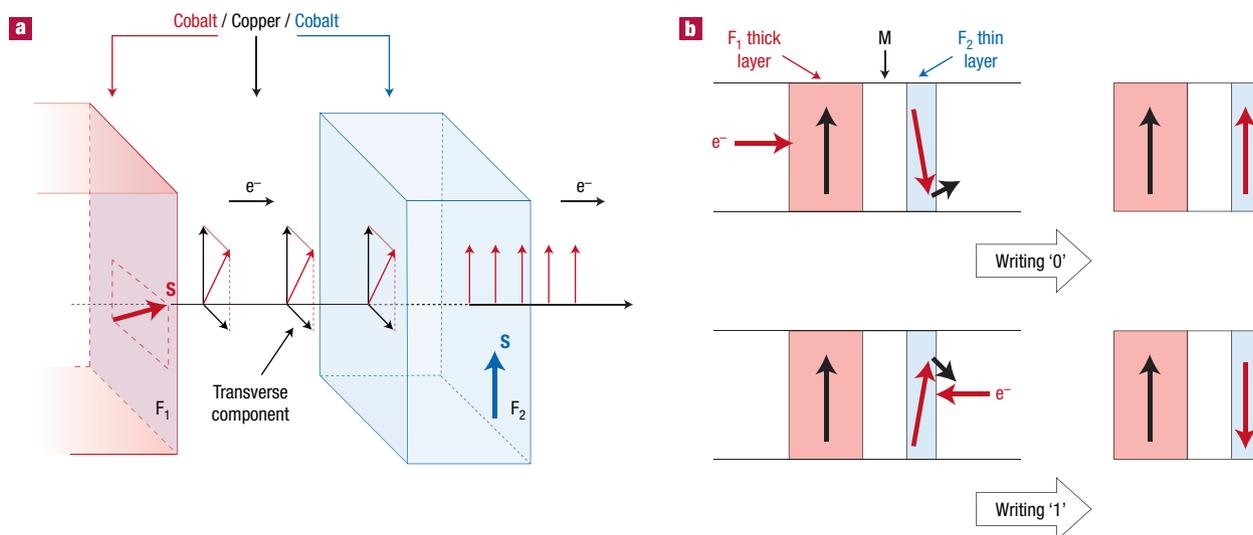
Figure 6 Spin-transfer switching. **a**, Principle of the STT effect, for a typical case of a Co(F1)/Cu/Co(F2) trilayer pillar. A current of *s* electrons flowing from left to right will acquire through F1 (assumed to be thick and acting as a spin polarizer) an average spin moment along the magnetization of F1. When the electrons reach F2, the *s*–*d* exchange interaction quickly aligns the average spin moment along the magnetization of F2. To conserve the total angular momentum, the transverse spin angular momentum lost by the electrons is transferred to the magnetization of F2, which senses a resulting torque tending to align its magnetization towards F1. **b**, Principle of STT writing of a MRAM cell: reversing the current flowing through the cell will induce either parallel or antiparallel orientation of the two ferromagnetic layers F1 and F2.

the polarizing layer, writing an antiparallel configuration beyond a threshold current density j_{C^-}.

Since the first observation on Co/Cu/Co trilayers, STT writing has been achieved on many different stacks, including exchange-bias pinned layers and SAF layers[67]. It also works with tunnel junctions[68], and in particular with MgO tunnel barriers[69]. Moreover, the threshold current densities are becoming nearly compatible with NMOS transistor output as predicted by the International Technology Roadmap for Semiconductors. And in the near future, TAS and STT writing modes could be combined for an even smaller switching current.

Companies have already presented several demonstrations of 'spin-RAM'[70,71]. As shown in Fig. 7, the cell structure has now become extremely simple, opening the way to high densities. Is it enough to compete with NAND Flash on mass data storage in standalone memories? In terms of areal density, Flash still offers a smaller multi-bit cell, and three-dimensional (3D) stacking has been announced[72]. But MRAM has other advantages, such as potentially infinite endurance (compared with ~10^5 cycles for a Flash) and potential for sub-nanosecond operation[66,73,74], that make it competitive as universal memory.

PERSPECTIVES

One grave limitation to ultra-high-density spin-MRAM is the requirement of one transistor per cell (1T/1MTJ). The cross-point memory architecture provides a way of reaching very high densities[75], lower fabrication costs and a potential for 3D stacking of several recording layers. Intermediate cell structures such as 1T/4MTJ[76] have also been proposed. Multi-level cell operation was also recently achieved in TAS-RAM[77]. But in all cases increased density is obtained at the expense of smaller signal amplitude and thus much slower read.

One step to fight these limitations, at least partially, would be to gain at least one order of magnitude in the amplitude of the magnetoresistance, moving towards a true 'current switch' with

$\Delta R/R$ values comparable, for example, to those of phase-change RAM (PCRAM). This could be achieved by replacing metallic ferromagnetic layers with 100% spin-polarized conductors such as half-metallic oxides[78] or Heussler alloys[79,80], or diluted magnetic semiconductors (DMS)[81,82]. DMS furthermore open the way to new effects such as tunnelling anisotropic magnetoresistance[83,84], and, in the long term, to quantum dot storage devices[85]. Another promising concept is that of the 'spin filter'[86] where tunnelling happens through a ferromagnetic barrier: the transmission varies exponentially with the square root of the barrier height, which itself depends on electron spin direction versus barrier magnetization. Such developments would of course also benefit HDD. Another approach is to build a three-terminal device that can produce both the transistor effect and magnetoresistance in a single magnetic device[87–89].

All these ideas show promising results at low temperature, but depend on materials issues such as obtaining Curie temperatures well above room temperature, mastering a complex stoichiometry (oxides, Heussler alloys) at an interface, or maintaining the fabrication thermal budget compatible with the CMOS process, though these new materials usually require specific high-temperature growth. Moreover, three-terminal devices can so far provide only very small currents (microamperes at most), below CMOS compatibility levels, and independent writing of one or two magnetic layers may prove difficult to scale down even using spin transfer.

Future magnetic mass storage could come instead from domain wall devices, in an approach conceptually close to that of the former 'bubble' magnetic memories[90]. File architecture for mass storage does not require random access to a single bit or word as proposed in spin-RAM, but can accommodate random access only to large sectors in which binary information is written or read sequentially, such as in HDD. A chain of domain walls in a magnetic stripe can indeed represent such a sector storing binary information, but a simple application of a uniform magnetic field would immediately destroy it by annihilating the reverse domain. It was first proposed[91,92] to use an oscillating magnetic field, uniform over the whole chip, acting on a specific domain wall circuit behaving as a shift register: the global
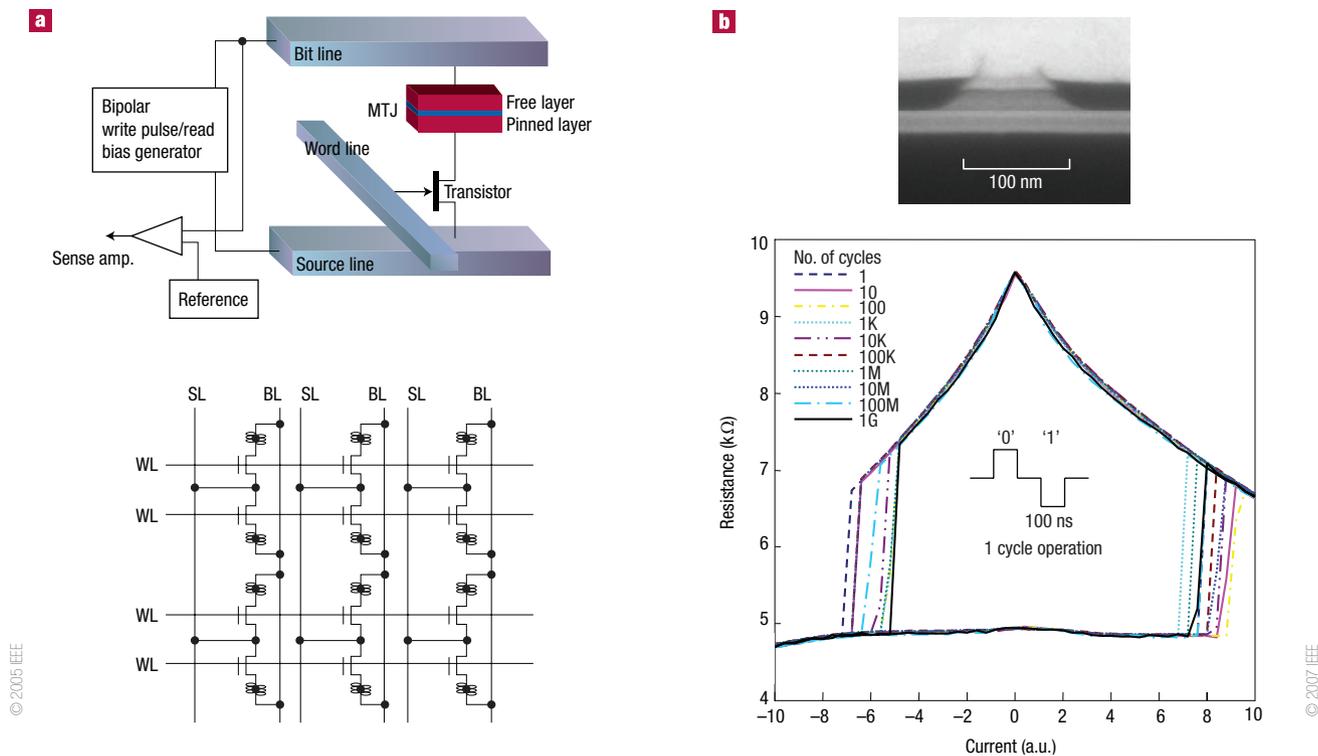
Figure 7 The spin-RAM. **a**, Schematic architecture of a spin-RAM; upper panel, scheme of the memory cell, and lower panel, tentative architecture of the cell array. Reprinted with permission from ref. 70. **b**, Resistance versus current hysteresis loop of a spin-RAM cell. Reprinted with permission from ref. 71. The different colours show the evolution of the loop after an increasing number (up to 1 G = 10^9) of writing cycles (100 ns pulses of successively positive and negative currents, see image). This demonstrates excellent stability. TEM image: TMR device size 100 nm × 50 nm; free layer CoFe (1.0 nm) / NiFe (2.0 nm); tunnel barrier MgO (1.0 nm).

character of the applied field makes downscaling and 3D stacking achievable[93]. Even more promising for very-high-density solid-state integration, a current injected in the magnetic stripe applies the same pressure to all domain walls along the direction of electron travel, propagating the walls simultaneously at the same speed, without losing information. This mimics the fast passing of bits in front of the head in HDD recording, but here there is no moving part (hence increased ruggedness) and addressing a sector would be done by CMOS electronics with microsecond access times. This scheme thus opens the way to very compact 'storage track memory devices'[94], and could also be used in a new kind of MRAM[95] (Fig. 8). But many advances are needed before its practical implementation.

The theory mixes spin transfer torque (electrons crossing a domain wall transfer spin angular momentum to the non-uniform magnetization in the wall) and mechanical momentum transfer (electrons are reflected from narrow walls), leading to a domain wall propagation controlled with a current density beyond a threshold[96,97]. The effect has indeed been observed in metals magnetized in plane[98,99] and perpendicular to plane[100], or in DMS[101] (with orders of magnitude lower currents but much higher resistance and other problems). However, even qualitative agreement between experience and theory is not straightforward[102,103].

On the experimental aspect, crucial progress has to be made in reliably controlling domain wall propagation with low current densities. First non-volatile reliable trapping of the domain walls must be provided at dedicated positions in the 'data sector'. Most works use simple notches[104,105], but more elaborate pinning profiles have also been proposed[106,107]. But not much has been published on the evolution of the thermal stability of the pinning when downscaling the dimensions. Besides, even in a parallel stripe and even more at

artificial notches with a distribution of patterning defects, domain walls can take different structures that are close in energy, and may even change structure under a current pulse[105,108–110]. This is a potential problem for reliable operation, because the parameters of current-induced propagation should depend on the wall structure. Last but not least, the threshold current density necessary to depin a domain wall from a trap, or even to start motion in a parallel stripe, is still too high for applications (above a few 10^6 A cm^{-2}). Great progress has recently been made by using the natural radiofrequency dynamics of a domain wall pinned in a potential well[111–113]. Note, however, that if the current density is still too high, the cross-section of a thin-film stripe is intrinsically small so the threshold current is already much smaller than is available from the smallest CMOS transistors, a key asset for developing low-power data-storage devices (Fig. 8b). Finally, the achievable domain wall speed is also a crucial issue for fast data rates[114–117]. For instance, with maximum domain wall speed around 100 m s^{-1} and an on-track linear density of one domain wall every 200 nm, already very demanding values, the data rate would be around 0.5 Gbit s^{-1}. This would be in line with today's HDD data rates, but is far from being demonstrated.

In the long term, even higher densities could be reached by replacing domain walls by smaller magnetization vortices[118], in a trend similar to that from bubble to Bloch line memories[90].

We have tried in this review to share our amazement at the outstanding progress in spin electronics over the past two decades, under the convergence of a chain of scientific breakthroughs and technology advances. If giant magnetoresistance opened the way in 1988 to control transport through magnetization, spin transfer now allows magnetization to be controlled through transport, closing the loop for a new paradigm, from magnetic recording to spin storage.
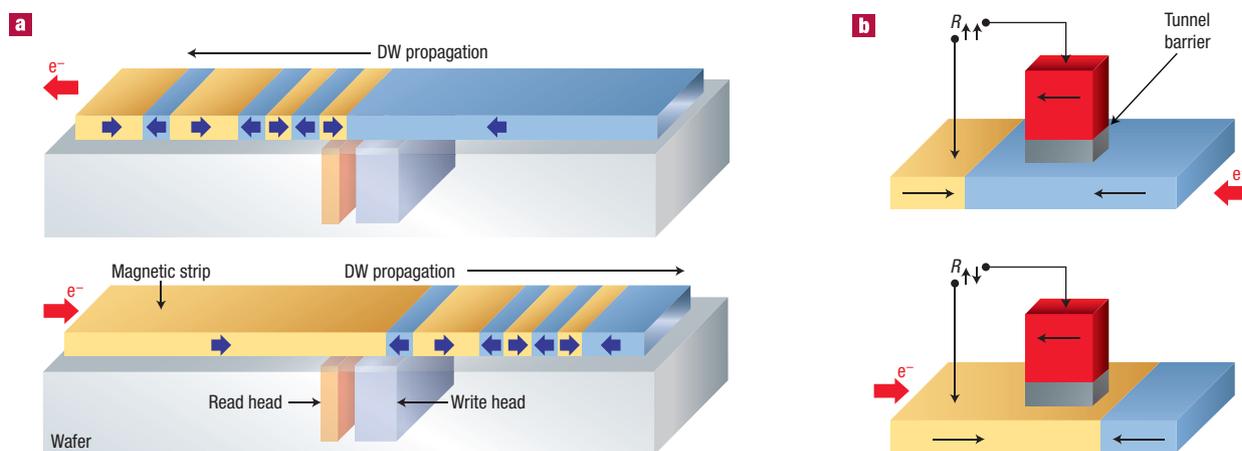
Figure 8 Domain wall storage devices. Examples of storage devices using current-induced domain wall (DW) propagation. **a**, In the concept first proposed by Parkin[94], the binary information is stored by a chain of domain walls in a magnetic stripe. An electrical current in the stripe, by applying the same pressure to all the domain walls, moves them simultaneously at the same speed for a sequential reading (or writing) at fixed read and write heads. A reverse current can move the domain walls in the opposite direction for resetting, or in an alternative solution the domain walls might turn on a loop. This mimics the fast passing of bits in front of the head in HDD recording, but here there is no moving part and addressing a sector would be done by CMOS electronics at microsecond access times. The initial scheme[94] proposes to store data in vertical stripes: this would open the way to very compact high capacity 'storage track memory devices'. Other schemes now propose multilayers of in-plane domain tracks, which would be easier to fabricate. **b**, Scheme of a MRAM cell using domain wall propagation from one stable position to another on either side of a magnetic tunnel junction (ref. 95).

Traditional hard-disk recording has gained orders of magnitude in storage capacity, thus entering the consumer electronics markets. And the MRAM magnetic solid-state memory is now in production, although as yet only for niche markets.

But the intrinsic speed and endurance of magnetic recording, together with the potential of the spin-RAM to work with CMOS-compatible electrical parameters, could open the way to applications where data storage would not be the primary objective although non-volatility would still be a key asset. Along this line, it has been proposed that logic calculations through magnetic interactions could be performed, in magnetic quantum cellular automata[119,120], or in domain wall logic[92], for low-power massively parallel logic operations under a uniform cyclical magnetic field. MTJs can also be used for logic calculation, either directly[121] (a nice idea but one whose practical realization is uncertain) or by a dense integration of MTJs into CMOS logic circuits[122,123] where they bring instant ON/OFF, run time re-programmability, and overall improved operation safety. Magnetism would thus enter the realm of the CPU. But a great step forward would be to realize three-terminal spin electronic devices that would enable a complete programmable logic function to be packed into a single nanodevice. Let us assume a source–gate–drain device where the magnetization of magnetic source and drain could be independently controlled, injecting spin-polarized electrons into a channel of spin-dependent transmission that could also be controlled by a gate voltage. Such a device has multiple inputs to control a multi-level output, realizing a logic function that can be programmed through the non-volatile magnetic configurations. The first proposition of this kind[18], despite recent progress in injecting spin polarization into semiconductors[124], has not yet been achieved in practice. New concepts are being proposed[125–127], and more could be realized, for instance, with molecules[128–132]. In the longer term, the use of spin injection and spin currents[21,133] may lead to the development of 'spin logic' devices[134].

Ultimately, 'magnetic' writing will again become a problem in much smaller and more complex devices, and new routes will have to be found. As in nanoelectronics, zero-current, gate-voltage-controlled writing would be ideal. Preliminary results have recently been obtained by using interfacial coupling with piezoelectric or even multiferroic materials[135–137], or through electric field control of ferromagnetism in DMS[138,139]. In an even more futuristic approach, switching by spin currents only (no charge currents) has been announced[140], in a pioneering step towards nanoelectronics using spin currents only. As a whole, finding solutions to the magnetic writing problem may prove to be a key issue on the way to future spin electronics, as it has been for the past evolution of magnetic recording.

References

1. Moser, A. *et al.* Magnetic recording: advancing into the future. *J. Phys. D* **35,** R157–R167 (2002).
2. Mott, N. Electrons in transition metals. *Adv. Phys.* **13,** 325–422 (1964).
3. Fert, A. & Campbell, I. A. Two-current conduction in nickel. *Phys. Rev. Lett.* **21,** 1190–1192 (1968).
4. Fert, A. & Campbell, I. Electrical resistivity of ferromagnetic nickel and iron based alloys. *J. Phys. F* **6,** 849–871 (1976).
5. Fert, A., Duvail, J. & Valet, T. Spin relaxation effects in the perpendicular magnetoresistance of magnetic multilayers. *Phys. Rev. B* **52,** 6513–6521 (1995).
6. Baibich, M. N. *et al.* Giant magnetoresistance of (001)Fe/(001)Cr magnetic superlattices. *Phys. Rev. Lett.* **61,** 2472–2475 (1988).
7. Binasch, G., Grünberg, P., Saurenbach, F. & Zinn, W. Enhanced magnetoresistance in layered magnetic structures with antiferromagnetic interlayer exchange. *Phys. Rev. B* **39,** 4828–4830 (1989).
8. Levy, P. M. & Mertig, I. in *Spin Dependent Transport in Magnetic Nanostructures* (eds Maekawa, S. & Shinjo, T.) Ch. 2, 47-112 (CRC, Boca Raton, 2002).
9. Fert, A., Barthélémy, A. & Petroff, F. in *Nanomagnetism: Ultrathin Films, Multilayers and Nanostructures* (eds Mills, D. M. & Bland, J. A. C.) Ch. 6 (Elsevier, Amsterdam, 2006).
10. Grünberg, P. Magnetic field sensor with ferromagnetic thin layers having magnetically antiparallel polarized components. US patent 4,949,039 (1990).
11. Dieny, B. *et al.* Magnetoresistive sensor based on the spin valve effect. US patent 5,206,590 (1993).
12. Dieny, B. *et al.* Giant magnetoresistance in soft ferromagnetic multilayers. *Phys. Rev. B* **43,** 1297–1300 (1991).
13. Daughton, J. M. Magnetic tunneling applied to memory. *J. Appl. Phys.* **81,** 3758–3763 (1997).
14. Valet, T. & Fert, A. Theory of the perpendicular magnetoresistance in magnetic multilayers. *Phys. Rev. B* **48,** 7099–7113 (1993).
15. Schmidt, G., Ferrand, D., Molenkamp, L. W., Filip, A. T. & van Wees, B. J. Fundamental obstacle for electrical spin injection from a ferromagnetic metal into a diffusive semiconductor. *Phys. Rev. B* **62,** R4790–R4793 (2000).
16. Fert, A. & Jaffrès, H. Conditions for efficient spin injection from a ferromagnetic metal into a semiconductor. *Phys. Rev. B* **64,** 184420 (2001).
17. Jedema, F. J., Filip, A. T. & van Wees, B. J. Electrical spin injection and accumulation at room temperature in an all-metal mesoscopic spin valve. *Nature* **410,** 345–348 (2001).
18. Datta, S. & Das, B. Electronic analog of the electro-optic modulator. *Appl. Phys. Lett.* **56,** 665–667 (1990).
19. Gijs, M. A. M., Lenczowski, S. K. J. & Giesbers, J. B. Perpendicular giant magnetoresistance of microstructured Fe/Cr magnetic multilayers from 4.2 to 300 K. *Phys. Rev. Lett.* **70,** 3343–3346 (1993).

20. Bass, J. & Pratt, W. P. Current-perpendicular (CPP) magnetoresistance in magnetic metallic multilayers. *J. Magn. Magn. Mater.* **200,** 274–289 (1999).

21. Fert, A. & Piraux, L. Magnetic nanowires. *J. Magn. Magn. Mater.* **200,** 338–358 (1999).

22. Takagishi, M. *et al.* The applicability of CPP-GMR heads for magnetic recording. *IEEE Trans. Magn.* **38,** 2277–2282 (2002).

23. Childress, J. *et al.* Fabrication and recording study of all-metal dual-spin-valve CPP read heads. *IEEE Trans. Magn.* **42,** 2444–2446 (2006).

24. Jullière, M. Tunneling between ferromagnetic films. *Phys. Lett. A* **54,** 225–226 (1975).

25. Moodera, J. S., Kinder, L. R., Wong, T. M. & Meservey, R. Large magnetoresistance at room temperature in ferromagnetic thin film tunnel junctions. *Phys. Rev. Lett.* **74,** 3273–3276 (1995).

26. Miyazaki, T. & Tezuka, N. Giant magnetic tunneling effect in Fe/Al$_2$O$_3$/Fe junction. *J. Magn. Magn. Mater.* **139,** L231-L234 (1995).

27. Parkin, S. S. P. *et al.* Giant tunnelling magnetoresistance at room temperature with MgO (100) tunnel barriers. *Nature Mater.* **3,** 862–867 (2004).

28. Yuasa, S., Nagahama, T., Fukushima, A., Suzuki, Y. & Ando, K. Giant room-temperature magnetoresistance in single-crystal Fe/MgO/Fe magnetic tunnel junctions. *Nature Mater.* **3,** 868–871 (2004).

29. Butler, W. H., Zhang, X., Schulthess, T. C. & MacLaren, J. M. Spin-dependent tunneling conductance of Fe/MgO/Fe sandwiches. *Phys. Rev. B* **63,** 054416 (2001).

30. Mathon, J. & Umerski, A. Theory of tunneling magnetoresistance of an epitaxial Fe/MgO/Fe(001) junction. *Phys. Rev. B* **63,** 220403 (2001).

31. Lee, Y. M., Hayakawa, J., Ikeda, S., Matsukura, F. & Ohno, H. Effect of electrode composition on the tunnel magnetoresistance of pseudo-spin-valve magnetic tunnel junction with a MgO tunnel barrier. *Appl. Phys. Lett.* **90,** 212507 (2007).

32. Mao, S. *et al.* Commercial TMR heads for hard disk drives: characterization and extendibility at 300 gbit/in^2. *IEEE Trans. Magn.* **42,** 97–102 (2006).

33. Engel, B. *et al.* A 4-Mb toggle MRAM based on a novel bit and switching method. *IEEE Trans. Magn.* **41,** 132–136 (2005).

34. DeBrosse, J. *et al.* A high-speed 128-kb MRAM core for future universal memory applications. *IEEE J. Solid-State Circ.* **39,** 678–683 (2004).

35. Brown, W. F. Thermal fluctuations of a single-domain particle. *Phys. Rev.* **130,** 1677–1686 (1963).

36. Néel, L. Anisotropie superficielle et surstructures d'orientation magnétique. *J. Phys. Rad.* **15,** 225–239 (1954).

37. Gradmann, U. & Müller, J. Flat ferromagnetic, epitaxial 48Ni/52Fe(111) films of few atomic layers. *Phys. Status Solidi B* **27,** 313–324 (1968).

38. Carcia, P. F., Meinhaldt, A. D. & Suna, A. Perpendicular magnetic anisotropy in Pd/Co thin film layered structures. *Appl. Phys. Lett.* **47,** 178–180 (1985).

39. Chappert, C., Renard, D., Beauvillain, P. & Renard, J. Ferromagnetism of very thin films of nickel and cobalt. *J. Magn. Magn. Mater.* **54–57,** 795–796 (1986).

40. Daalderop, G. H. O., Kelly, P. J. & den Broeder, F. J. A. Prediction and confirmation of perpendicular magnetic anisotropy in Co/Ni multilayers. *Phys. Rev. Lett.* **68,** 682–685 (1992).

41. Meiklejohn, W. H. & Bean, C. P. New magnetic anisotropy. *Phys. Rev.* **102,** 1413–1414 (1956).

42. Nogues, J. *et al.* Exchange bias in nanostructures. *Phys. Rep.* **422,** 65–117 (2005).

43. Prejbeanu, I. *et al.* Thermally assisted switching in exchange-biased storage layer magnetic tunnel junctions. *IEEE Trans. Magn.* **40,** 2625–2627 (2004).

44. Skumryev, V. *et al.* Beating the superparamagnetic limit with exchange bias. *Nature* **423,** 850–853 (2003).

45. Grünberg, P., Schreiber, R., Pang, Y., Brodsky, M. B. & Sowers, H. Layered magnetic structures: evidence for antiferromagnetic coupling of Fe layers across Cr interlayers. *Phys. Rev. Lett.* **57,** 2442–2445 (1986).

46. Majkrzak, C. F. *et al.* Observation of a magnetic antiphase domain structure with long-range order in a synthetic Gd-Y superlattice. *Phys. Rev. Lett.* **56,** 2700–2703 (1986).

47. Parkin, S. S. P., More, N. & Roche, K. P. Oscillations in exchange coupling and magnetoresistance in metallic superlattice structures: Co/Ru, Co/Cr, and Fe/Cr. *Phys. Rev. Lett.* **64,** 2304–2307 (1990).

48. Bruno, P. & Chappert, C. Oscillatory coupling between ferromagnetic layers separated by a nonmagnetic metal spacer. *Phys. Rev. Lett.* **67,** 1602–1605(1991).

49. Bruno, P. Theory of interlayer magnetic coupling. *Phys. Rev. B* **52,** 411–439 (1995).

50. Margulies, D. T., Berger, A., Moser, A., Schabes, M. E. & Fullerton, E. E. The energy barriers in antiferromagnetically coupled media. *Appl. Phys. Lett.* **82,** 3701–3703 (2003).

51. Savchenko, L., Engel, B. N., Rizzo, N. D., Deherrera, M. F. & Janesky J. A. Method of writing to scalable magnetoresistance random access memory element. US patent 6,545,906B1 (2003).

52. Weller, D. *et al.* High K$_u$ materials approach to 100 Gbits/in^2. *IEEE Trans. Magn.* **36,** 10–15 (2000).

53. Durlam, M. *et al.* Low power 1 Mbit MRAM based on 1T1MTJ bit cell integrated with copper interconnects. *Symp. VLSI Techn. Dig.,* 158–161 (2002).

54. Worledge, D. C. Spin flop switching for magnetic random access memory. *Appl. Phys. Lett.* **84,** 4559–4561 (2004).

55. Daughton, J. M. & Pohm, A. V. Design of Curie point written magnetoresistance random access memory cells. *J. Appl. Phys.* **93,** 7304–7306 (2003).

56. Rizzo, N. D. & Engel, B. N. MRAM write apparatus and method. US patent 6,351,409 (2002).

57. Thirion, C., Wernsdorfer, W. & Mailly, D. Switching of magnetization by nonlinear resonance studied in single nanoparticles. *Nature Mater.* **2,** 524–527 (2003).

58. Nembach, H. T. *et al.* Microwave assisted switching in a Ni$_{81}$Fe$_{19}$ ellipsoid. *Appl. Phys. Lett.* **90,** 062503 (2007).

59. Slonczewski, J. Current-driven excitation of magnetic multilayers. *J. Magn. Magn. Mater.* **159,** L1-L7 (1996).

60. Berger, L. Emission of spin waves by a magnetic multilayer traversed by a current. *Phys. Rev. B* **54,** 9353–9358 (1996).

61. Albert, F. J., Katine, J. A., Buhrman, R. A. & Ralph, D. C. Spin-polarized current switching of a Co thin film nanomagnet. *Appl. Phys. Lett.* **77,** 3809–3811 (2000).

62. Berger, L. Prediction of a domain-drag effect in uniaxial, non-compensated, ferromagnetic metals. *J. Phys. Chem. Solids* **35,** 947–956 (1974).

63. Freitas, P. P. & Berger, L. Observation of s–d exchange force between domain walls and electric current in very thin Permalloy films. *J. Appl. Phys.* **57,** 1266–1269 (1985).

64. Slonczewski, J. C. Conductance and exchange coupling of two ferromagnets separated by a tunneling barrier. *Phys. Rev. B* **39,** 6995–7002 (1989).

65. Stiles, M. & Miltat, J. in *Spin Dynamics in Confined Magnetic Structures III* (eds Hillebrands, B. & Thiaville, A.) (Springer, Berlin, 2006)

66. Sun, J. Z. Spin–current interaction with a monodomain magnetic body: a model study. *Phys. Rev. B* **62,** 570–578 (2000).

67. Ralph, D. & Buhrman, R., in *Concepts in Spintronics* (ed. Maekawa, S.) (Oxford Univ. Press, 2006)

68. Huai, Y., Albert, F., Nguyen, P., Pakala, M. & Valet, T. Observation of spin-transfer switching in deep submicron-sized and low-resistance magnetic tunnel junctions. *Appl. Phys. Lett.* **84,** 3118–3120 (2004).

69. Hayakawa, J. *et al.* Current-induced magnetization switching in MgO barrier based magnetic tunnel junctions with CoFeB/Ru/CoFeB synthetic ferrimagnetic free layer. *Jpn. J. Appl. Phys.* **45,** L1057–L1060 (2006).

70. Hosomi, M. *et al.* Novel nonvolatile memory with spin torque transfer magnetization switching: spin-ram. *IEDM Tech. Dig.* 459–462 (2005).

71. Kawahara, T. *et al.* 2Mb spin-transfer torque RAM (SPRAM) with bit-by-bit bidirectional current write and parallelizing-direction current read. *ISSCC Dig. Tech. Papers,* 480–481 (2007).

72. Jung, S. *et al.* Three dimensionally stacked NAND Flash memory technology using stacking single crystal Si layers on ILD and TANOS structure for beyond 30 nm node. *IEDM Tech. Dig.,* 1–4 (2006).

73. Ito, K., Devolder, T., Chappert, C., Carey, M. J. & Katine, J. A. Micromagnetic simulation of spin transfer torque switching combined with precessional motion from a hard axis magnetic field. *Appl. Phys. Lett.* **89,** 252509 (2006).

74. Devolder, T., Chappert, C. & Ito, K. Sub-ns spin-transfer switching: compared benefits of free layer biasing and pinned layer biasing. *Phys. Rev. B* **75,** 224430 (2007).

75. Sakimura, N. *et al.* A 512 kb cross-point cell MRAM. *ISSCC Dig. Tech. Papers,* 278–279 (2003).

76. Tanizaki, H. *et al.* A high-density and high-speed 1T-4MTJ MRAM with voltage offset self-reference sensing scheme. *Asian Solid-State Circuits Conf. Dig. Tech. Papers,* 303–306 (2006).

77. Leuschner, R. *et al.* Thermal select MRAM with a 2-bit cell capability for beyond 65 nm technology node. *IEDM Tech. Dig.,* 1–4 (2006).

78. Bowen, M. *et al.* Nearly total spin polarization in La$_{2/3}$Sr$_{1/3}$MnO$_3$ from tunnelling experiments. *Appl. Phys. Lett.* **82,** 233–235 (2003).

79. Ishikawa, T. *et al.* Spin-dependent tunneling characteristics of fully epitaxial magnetic tunneling junctions with a full-Heusler alloy Co$_2$MnSi thin film and a MgO tunnel barrier. *Appl. Phys. Lett.* **89,** 192505 (2006).

80. Marukame, T., Ishikawa, T., Matsuda, K., Uemura, T. & Yamamoto, M. High tunnel magnetoresistance in fully epitaxial magnetic tunnel junctions with a full-Heusler alloy Co$_2$Cr$_{0.6}$Fe$_{0.4}$Al thin film. *Appl. Phys. Lett.* **88,** 262503 (2006).

81. Chiba, D., Sato, Y., Kita, T., Matsukura, F. & Ohno, H. Current-driven magnetization reversal in a ferromagnetic semiconductor (Ga,Mn)As/GaAs/(Ga,Mn)As tunnel junction. *Phys. Rev. Lett.* **93,** 216602 (2004).

82. Elsen, M. Spin transfer experiments on (Ga,Mn)As/(In,Ga)As/(Ga,Mn)As tunnel junctions. *Phys. Rev. B* **73,** 035303 (2006).

83. Gould, C. Tunneling anisotropic magnetoresistance: a spin-valve-like tunnel magnetoresistance using a single magnetic layer. *Phys. Rev. Lett.* **93,** 117203 (2004).

84. Gould, C., Schmidt, G. & Molenkamp, L. W. Tunneling anisotropic magnetoresistance-based devices. *IEEE Trans. Electron Dev.* **54,** 977–983 (2007).

85. Enaya, H., Semenov, Y. G., Kim, K. W. & Zavada, J. M. Electrical manipulation of nonvolatile spin cell based on diluted magnetic semiconductor quantum dots. *IEEE Trans. Electron Dev.* **54,** 1032–1039 (2007).

86. LeClair, P. *et al.* Large magnetoresistance using hybrid spin filter devices. *Appl. Phys. Lett.* **80,** 625–627 (2002).

87. Monsma, D. J., Lodder, J. C., Popma, T. J. A. & Dieny, B. Perpendicular hot electron spin-valve effect in a new magnetic field sensor: the spin-valve transistor. *Phys. Rev. Lett.* **74,** 5260–5263 (1995).

88. van Dijken, S., Jiang, X. & Parkin, S. S. P. Room temperature operation of a high output current magnetic tunnel transistor. *Appl. Phys. Lett.* **80,** 3364–3366 (2002).

89. Hehn, M., Montaigne, F. & Schuhl, A. Hot-electron three-terminal devices based on magnetic tunnel junction stacks. *Phys. Rev. B* **66,** 144411 (2002).

90. Hubert, A. & Schäfer, R. *Magnetic Domains* (Springer, Berlin, 1998).

91. Allwood, D. A. *et al.* Submicrometer ferromagnetic NOT gate and shift register. *Science* **296,** 2003–2006 (2002).

92. Allwood, D. A. *et al.* Magnetic domain-wall logic. *Science* **309,** 1688–1692 (2005).

93. Cowburn, R. P. & Allwood, D. A. Multiple layer magnetic logic memory device. UK patent GB2,430,318A (2007).

94. Parkin, S. S. P. Shiftable magnetic shift register and method using the same. US patent 6,834,005B1 (2004).

95. Cros, V., Grollier, J., Munoz Sanchez, M., Fert, A. & Nguyen Van Dau, F. Spin electronics device. Patent WO 2006/064022 (2006).

96. Tatara, G. & Kohno, H. Theory of current-driven domain wall motion: spin transfer versus momentum transfer. *Phys. Rev. Lett.* **92,** 086601 (2004).

97. Li, Z. & Zhang, S. Domain-wall dynamics and spin-wave excitations with spin-transfer torques. *Phys. Rev. Lett.* **92,** 207203 (2004).

98. Grollier, J. *et al.* Switching a spin valve back and forth by current-induced domain wall motion. *Appl. Phys. Lett.* **83,** 509 (2003).

99. Yamaguchi, A. *et al.* Real-space observation of current-driven domain wall motion in submicron magnetic wires. *Phys. Rev. Lett.* **92,** 077205 (2004).

100. Ravelosona, D., Lacour, D., Katine, J. A., Terris, B. D. & Chappert, C. Nanometer scale observation of high efficiency thermally assisted current-driven domain wall depinning. *Phys. Rev. Lett.* **95,** 117203 (2005).

101. Yamanouchi, M., Chiba, D., Matsukura, F. & Ohno, H. Current-induced domain-wall switching in a ferromagnetic semiconductor structure. *Nature* **428,** 539–542 (2004).

102. Thiaville, A., Nakatani, Y., Miltat, J. & Suzuki, Y. Micromagnetic understanding of current-driven domain wall motion in patterned nanowires. *Europhys. Lett.* **69,** 990–996 (2005).

103. Piechon, F. & Thiaville, A. Spin transfer torque in continuous textures: Semiclassical Boltzmann approach. *Phys. Rev. B* **75,** 174414 (2007).
104. Himeno, A. *et al.* Dynamics of a magnetic domain wall in magnetic wires with an artificial neck. *J. Appl. Phys.* **93,** 8430–8432 (2003).
105. Hayashi, M. *et al.* Dependence of current and field driven depinning of domain walls on their structure and chirality in permalloy nanowires. *Phys. Rev. Lett.* **97,** 207205 (2006).
106. Allwood, D. A., Xiong, G. & Cowburn, R. P. Domain wall diodes in ferromagnetic planar nanowires. *Appl. Phys. Lett.* **85,** 2848–2853 (2004).
107. Faulkner, C. C. *et al.* Artificial domain wall nanotraps in $Ni_{81}Fe_{19}$ wires. *J. Appl. Phys.* **95,** 6717–6719 (2004).
108. Klaui, M. *et al.* Direct observation of domain-wall configurations transformed by spin currents. *Phys. Rev. Lett.* **95,** 026601 (2005).
109. Klaui, M. *et al.* Current-induced vortex nucleation and annihilation in vortex domain walls. *Appl. Phys. Lett.* **88,** 232507 (2006).
110. He, J., Li, Z. & Zhang, S. Current-driven vortex domain wall dynamics by micromagnetic simulations. *Phys. Rev. B* **73,** 184408 (2006).
111. Saitoh, E., Miyajima, H., Yamaoka, T. & Tatara, G. Current-induced resonance and mass determination of a single magnetic domain wall. *Nature* **432,** 203–206 (2004).
112. Thomas, L. *et al.* Oscillatory dependence of current-driven magnetic domain wall motion on current pulse length. *Nature* **443,** 197–200 (2006).
113. Thomas, L. *et al.* Resonant amplification of magnetic domain-wall motion by a train of current pulses. *Science* **315,** 1553–1556 (2007).
114. Nakatani, Y., Thiaville, A. & Miltat, J. Faster magnetic walls in rough wires. *Nature Mater.* **2,** 521–523 (2003).
115. Lim, C. K. *et al.* Domain wall displacement induced by subnanosecond pulsed current. *Appl. Phys. Lett.* **84,** 2820–2822 (2004).
116. Hayashi, M. *et al.* Current driven domain wall velocities exceeding the spin angular momentum transfer rate in permalloy nanowires. *Phys. Rev. Lett.* **98,** 037204. (2007).
117. Yamanouchi, M., Chiba, D., Matsukura, F., Dietl, T. & Ohno, H. Velocity of domain-wall motion induced by electrical current in the ferromagnetic semiconductor (Ga,Mn)As. *Phys. Rev. Lett.* **96,** 096601 (2006).
118. Kasai, S., Nakatani, Y., Kobayashi, K., Kohno, H. & Ono, T. Current-driven resonant excitation of magnetic vortices. *Phys. Rev. Lett.* **97,** 107204 (2006).
119. Cowburn, R. P. & Welland, M. E. Room temperature magnetic quantum cellular automata. *Science* **287,** 1466–1468 (2000).
120. Imre, A. *et al.* Majority logic gate for magnetic quantum-dot cellular automata. *Science* **311,** 205–208 (2006).
121. Ney, A., Pampuch, C., Koch, R. & Ploog, K. H. Programmable computing with a single magnetoresistive element. *Nature* **425,** 485–487 (2003).
122. Black, W. C. J. & Das, B. Programmable logic using giant-magnetoresistance and spin-dependent tunneling devices. *J. Appl. Phys.* **87,** 6674–6679 (2000).
123. Zhao, W. *et al.* Integration of Spin-RAM technology in FPGA circuits. *Proc. ICSICT* 799–802 (2006).
124. Min, B., Motohashi, K., Lodder, C. & Jansen, R. Tunable spin-tunnel contacts to silicon using low-work-function ferromagnets. *Nature Mater.* **5,** 817–822 (2006).
125. Hall, K. C., Lau, W. H., Gundogdu, K., Flatte, M. E. & Boggess, T. F. Nonmagnetic semiconductor spin transistor. *Appl. Phys. Lett.* **83,** 2937–2939 (2003).
126. Hall, K. C. & Flatte, M. E. Performance of a spin-based insulated gate field effect transistor. *Appl. Phys. Lett.* **88,** 162503 (2006).
127. Tanaka, M. & Sugahara, S. MOS-based spin devices for reconfigurable logic. *IEEE Trans. Electron Dev.* **54,** 961–976 (2007).
128. Pasupathy, A. N. *et al.* The Kondo effect in the presence of ferromagnetism. *Science* **306,** 86–89 (2004).
129. Sahoo, S., Kontos, T., Schonenberger, C. & Surgers, C. Electrical spin injection in multiwall carbon nanotubes with transparent ferromagnetic contacts. *Appl. Phys. Lett.* **86,** 112109 (2005).
130. Hueso, L. E. *et al.* Transformation of spin information into large electrical signals using carbon nanotubes. *Nature* **445,** 410–413 (2007).
131. Romeike, C., Wegewijs, M. R., Ruben, M., Wenzel, W. & Schoeller, H. Charge-switchable molecular magnet and spin blockade of tunneling. *Phys. Rev. B* **75,** 064404 (2007).
132. Fert, A., George, J., Jaffres, H. & Mattana, R. Semiconductors between spin-polarized sources and drains. *IEEE Trans. Electron Dev.* **54,** 921–932 (2007).
133. Kimura, T., Hamrle, J. & Otani, Y. Estimation of spin-diffusion length from the magnitude of spin-current absorption: multiterminal ferromagnetic/nonferromagnetic hybrid structures. *Phys. Rev. B* **72,** 014461 (2005).
134. Dery, H., Dalal, P., Cywinski, L. & Sham, L. J. Spin-based logic in semiconductors for reconfigurable large-scale circuits. *Nature* **447,** 573–576 (2007).
135. Khomskii, D. Multiferroics: Different ways to combine magnetism and ferroelectricity. *J. Magn. Magn. Mater.* **306,** 1–8 (2006).
136. Zavaliche, F. *et al.* Electric field-induced magnetization switching in epitaxial columnar nanostructures. *Nano Lett.* **5,** 1793–1796 (2005).
137. Zhao, T. *et al.* Electrical control of antiferromagnetic domains in multiferroic $BiFeO_3$ films at room temperature. *Nature Mater.* **5,** 823–829 (2006).
138. Chiba, D., Matsukura, F. & Ohno, H. Electric-field control of ferromagnetism in (Ga,Mn)As. *Appl. Phys. Lett.* **89,** 162505 (2006).
139. Wunderlich, J. *et al.* Coulomb blockade anisotropic magnetoresistance effect in a (Ga,Mn)As single-electron transistor. *Phys. Rev. Lett.* **97,** 077201 (2006).
140. Kimura, T., Otani, Y. & Hamrle, J. Switching magnetization of a nanoscale ferromagnetic particle using nonlocal spin injection. *Phys. Rev. Lett.* **96,** 037201 (2006).